

Hund's-Rule Coupling Effect in Itinerant Ferromagnetism

Takuya OKABE

Department of Physics, Kyoto University, Kyoto 606-01

(Received November 30, 1996)

We present a general model which includes the ferromagnetic Kondo lattice and the Hubbard model as special cases. The stability of the ferromagnetic state is investigated variationally. We discuss the mechanism of ferromagnetism in metallic nickel, emphasizing the importance of orbital degeneracy and the effect of the Hund's-rule coupling.

§1. Introduction

The study of itinerant ferromagnetism is one of the most difficult problems in solid-state theory. In the 1960's, this problem was studied for the single-band Hubbard model by Kanamori,¹⁾ Gutzwiller²⁾ and Hubbard.³⁾ In the Hubbard model, it is now widely known that the ferromagnetic ground state is realized only in exceptional situations. An example is the Nagaoka ferromagnetic state,⁴⁾ which is shown to be the exact ground state when a single carrier is doped in the half-filled $U = \infty$ Hubbard model. The other cases were discussed by Tasaki and Mielke,⁵⁾ who investigated the model in which the relevant band is flat or almost flat. Furthermore, Penc et al.⁶⁾ discussed ferromagnetism in such a way that their formulation includes flat-band limit as a special case. Our theory presented here is also aimed at generalizing the model for itinerant ferromagnetism so as to include the Nagaoka state in the Hubbard model. Our generalization is made by including the effect of the Hund's-rule coupling, rather than by considering the specific lattice structure.^{6),7)}

In a pioneering work on the electron correlation effect, Kanamori¹⁾ discussed ferromagnetism of Ni. Although he started with degenerate $3d$ bands, he finally reduced the problem to that of a single band model. This is partly due to overestimation of the interaction energy, which was regarded as being roughly twice as large as the band width. With respect to this point, it is now commonly accepted that the interaction energy and the band width in Ni are of the same order of magnitude.^{8),9),10)} Therefore, it is necessary to reconsider the effect of the Hund's-rule coupling.

In ferromagnetic nickel, satellite structure was observed at 6 eV below the Fermi energy.^{11),12),13),14)} This structure is interpreted as a two-hole bound state.^{15),16)} To reproduce the structure, one must take into account electron-electron and electron-hole multiple scattering effects. For this purpose, formal treatments have been given by many authors,^{17),18),19),20),21)} and the resulting mathematical expressions are all in similar forms. In conformity with these results, several works have been presented to explain the structure.^{22),23),24)} The conclusion is that it can be explained in the single-band model if one assumes the Hubbard repulsion $U \lesssim W \sim 4$ eV.^{15),16),24)} However, it then becomes difficult to maintain the complete ferromagnetic ground

state for such a small value of U .^{21),24)} Therefore the effect of degenerate d -orbitals and the Hund's-rule coupling should be considered.

We investigated itinerant ferromagnetism in $3d$ transition metal systems in the generalized Gutzwiller approximation,²⁵⁾ and concluded that the atomic correlation effect is quite effective in realizing ferromagnetism in Ni. In this paper, more precise discussion on the local stability condition of the complete ferromagnetic state is given. We restrict our argument to absolute zero temperature. Not only the longitudinal but also transverse component of the Hund's-rule coupling is taken into account. We reproduce the theoretical expressions derived for the Hubbard model by considering the multiple magnon scattering effect^{17),19),20),21)} as a special case of our general result.

In the next section, we present a general model to treat itinerant ferromagnetism. The model includes the ferromagnetic Kondo lattice model, which was treated in our previous paper.²⁶⁾ In §§3 and 4, the formulae required in the following sections are derived. As an example, we discuss a two-band model, which consists of a pair of Hubbard models coupled by the Hund's-rule coupling (§5). Then a simple theory for metallic nickel is given in §6. It is concluded that the Hund's-rule coupling effect is indispensable. Conclusion is given in the last section, §7.

§2. General model for the itinerant ferromagnet

As a general model for an itinerant ferromagnet, we begin with the Hamiltonian

$$H = T + V, \quad (2.1)$$

$$T = - \sum_{i,j,\mu,\nu,\sigma} t_{ij}^{\mu\nu} c_{i\mu\sigma}^\dagger c_{j\nu\sigma},$$

$$V = U \sum_{i,\mu} \hat{n}_{i\mu\uparrow} \hat{n}_{i\mu\downarrow} + U' \sum_{i,<\mu\neq\nu>} \hat{n}_{i\mu} \hat{n}_{i\nu} - J \sum_{i,<\mu\neq\nu>} \mathbf{s}_{i\mu} \cdot \mathbf{s}_{i\nu}, \quad (2.2)$$

where

$$\begin{aligned} \hat{n}_{i\mu\sigma} &\equiv c_{i\mu\sigma}^\dagger c_{i\mu\sigma}, \\ \hat{n}_{i\mu} &\equiv \sum_{\sigma} \hat{n}_{i\mu\sigma}, \\ \mathbf{s}_{i\mu} &\equiv \frac{1}{2} \sum_{\sigma,\sigma'} c_{i\mu\sigma}^\dagger \boldsymbol{\sigma}_{\sigma,\sigma'} c_{i\mu\sigma'}, \end{aligned} \quad (2.3)$$

with the Pauli matrices $\boldsymbol{\sigma}$. The subscripts i, j and μ, ν designate lattice sites and localized orbitals, respectively. The summation with $\langle \mu \neq \nu \rangle$ denotes that the sum is taken over pairs of orbitals (μ, ν) .

For simplicity, we assume that each component of degenerate bands is labeled by the index μ , or $t_{ij}^{\mu\nu} = t_{ij}^\mu \delta_{\mu\nu}$. Then we have

$$T = \sum_{k,\mu,\sigma} \varepsilon_{k\mu} c_{k\mu\sigma}^\dagger c_{k\mu\sigma}, \quad (2.4)$$

where

$$\varepsilon_{k\mu} = - \sum_j t_{ij}^\mu e^{ik(r_j - r_i)}. \quad (2.5)$$

If we further assume a tight-binding band, or $t_{ij}^\mu = t_\mu$ for the nearest-neighbor pair i, j and zero for any other pairs $i \neq j$, we have

$$\varepsilon_{k\mu} = -t_\mu \sum_\delta e^{ik\delta} - t_{ii}^\mu, \quad (2.6)$$

where the summation is taken over the nearest neighbor vector δ . The second term is a constant shift of energy. In the following sections, we assume $t_{ii}^\mu = 0$ and use the μ -dependent Fermi energy $\varepsilon_{f\mu}$. Then,

$$\sum_k \varepsilon_{k\mu} = 0. \quad (2.7)$$

This assumption does not cause any difficulty since we are prohibiting the inter-band transfer of particles by the assumption made above (2.4).

The interaction part is rewritten as

$$\begin{aligned} V = & U \sum_{i,\mu} \hat{n}_{i\mu\uparrow} \hat{n}_{i\mu\downarrow} \\ & + (U' - \frac{J}{4}) \sum_{i, \langle \mu \neq \nu \rangle, \sigma} \hat{n}_{i\mu\sigma} \hat{n}_{i\nu\sigma} + (U' + \frac{J}{4}) \sum_{i, \mu \neq \nu} \hat{n}_{i\mu\uparrow} \hat{n}_{i\nu\downarrow} \\ & - \frac{J}{2} \sum_{i, \langle \mu \neq \nu \rangle} (s_{i\mu}^+ s_{i\nu}^- + s_{i\mu}^- s_{i\nu}^+), \end{aligned} \quad (2.8)$$

where

$$s_{i\mu}^\pm \equiv (\mathbf{s}_{i\mu})_x \pm i(\mathbf{s}_{i\mu})_y, \quad (2.9)$$

or, explicitly,

$$\begin{aligned} s_{i\mu}^+ &= c_{i\mu\uparrow}^\dagger c_{i\mu\downarrow}, \\ s_{i\mu}^- &= c_{i\mu\downarrow}^\dagger c_{i\mu\uparrow}. \end{aligned} \quad (2.10)$$

As the ferromagnetic ground state itself is well described by band theory,²⁷⁾ it is safely assumed that the electron correlation effect is irrelevant in the ferromagnetic state. In fact, this is true in the single-band Hubbard model, where the Pauli principle makes interaction irrelevant. If the complete ferromagnetic ground state is uncorrelated, an analytical treatment to estimate the elementary excitation energy becomes feasible. Therefore, for this purpose we assume $U' = J/4$. Then,

$$\begin{aligned} V = & U \sum_{i,\mu} \hat{n}_{i\mu\uparrow} \hat{n}_{i\mu\downarrow} \\ & - \frac{J}{2} \sum_{i, \langle \mu \neq \nu \rangle} \left(s_{i\mu}^+ s_{i\nu}^- + s_{i\mu}^- s_{i\nu}^+ - (\hat{n}_{i\mu\uparrow} \hat{n}_{i\nu\downarrow} + \hat{n}_{i\mu\downarrow} \hat{n}_{i\nu\uparrow}) \right). \end{aligned} \quad (2.11)$$

Finally we have two positive parameters U and J to describe the interaction effect. In our model, the term energy of the singlet state formed by two electrons in the same (different) orbital is U (J), while that of the triplet state is zero.²⁸⁾ For example, for metallic nickel, the relative order is $J \lesssim U \lesssim W \sim 4$ eV, where W is the band width. In the following sections, we investigate the model Hamiltonian which consists of (2.4) and (2.11), i.e.,

$$\begin{aligned} H &= T + V \\ &= \sum_{k,\mu,\sigma} \varepsilon_{k\mu} c_{k\mu\sigma}^\dagger c_{k\mu\sigma} + U \sum_{i,\mu} \hat{n}_{i\mu\uparrow} \hat{n}_{i\mu\downarrow} \\ &\quad - \frac{J}{2} \sum_{i, \langle \mu \neq \nu \rangle} \left(s_{i\mu}^+ s_{i\nu}^- + s_{i\mu}^- s_{i\nu}^+ - (\hat{n}_{i\mu\uparrow} \hat{n}_{i\nu\downarrow} + \hat{n}_{i\mu\downarrow} \hat{n}_{i\nu\uparrow}) \right). \end{aligned} \quad (2.12)$$

The complete ferromagnetic ground state $|\mathbb{F}\rangle$ is given by

$$|\mathbb{F}\rangle \equiv \prod_{\varepsilon_{k\mu} < \varepsilon_{f\mu}} c_{k\mu\uparrow}^\dagger |0\rangle, \quad (2.13)$$

where $|0\rangle$ denotes the vacuum and $\varepsilon_{f\mu}$ is the Fermi energy.

The above model contains several models which have been intensively discussed in the field of the itinerant ferromagnetism. For example, we recover the single-band Hubbard Hamiltonian by neglecting orbital degeneracy. On the other hand, we reproduce the ferromagnetic Kondo lattice model with the localized spin $S_f = D/2$. For this, we may assume $n_\mu = 1$ for bands with $\mu = 1, 2, 3, \dots, D$, and $n_{D+1} \equiv n$ for the conduction band ($0 \leq n \leq 1$). The completely filled band ($n_\mu = 1$) represents the Mott insulator and acts as an array of localized spins, $s_\mu = 1/2$. These localized spins are coupled to form $S_f = D/2$ by the on-site Hund's rule. To describe metallic nickel, one may assume triply-degenerate bands with $n_\mu = 0.2$ for $\mu = 1, 2$ and 3 (§6).

§3. Spin wave

In this and the next section we derive formulae required in the following sections. These are generalization of our previous results.²⁶⁾

3.1. Approximation I

First we consider the trial state for the spin-wave-excited state

$$\Psi_{0q} = \Lambda^{-1/2} \sum_i e^{iqr_i} S_i^- |\mathbb{F}\rangle, \quad (3.1)$$

where

$$S_i^- \equiv \sum_\mu s_{i\mu}^-, \quad (3.2)$$

and Λ is the total number of lattice sites. Description with this trial state corresponds to the random phase approximation (RPA) in the strong coupling limit.

The energy expectation value of (3.1) gives the magnon dispersion,²⁶⁾

$$\omega_{0q} = \frac{1}{2S} \cdot \frac{1}{\Lambda} \sum_{k,\mu} n_{k\mu} (\varepsilon_{k+q\mu} - \varepsilon_{k\mu}), \quad (3.3)$$

where

$$\begin{aligned} n_{k\mu} &= \langle \mathbf{F} | c_{k\mu\uparrow}^\dagger c_{k\mu\uparrow} | \mathbf{F} \rangle, \\ n_\mu &= \sum_k n_{k\mu}, \\ 2S &\equiv \sum_\mu n_\mu. \end{aligned} \quad (3.4)$$

In these expressions, $n_{k\mu}$ is the step function, n_μ is a carrier density in the band μ , and S represents the total spontaneous magnetization.

In the long wavelength limit, we have

$$\omega_{0q} = D_0 q^2 \equiv \sum_\mu D_{0\mu} q^2, \quad (q \rightarrow 0) \quad (3.5)$$

where

$$D_{0\mu} = \frac{|\epsilon_{g\mu}|}{2S z}, \quad (3.6)$$

and

$$\epsilon_{g\mu} \equiv \frac{1}{\Lambda} \sum_k n_{k\mu} \varepsilon_{k\mu}. \quad (3.7)$$

Here we have assumed a tight-binding band with the coordination number z . The negative quantity $\epsilon_{g\mu}$ is the total kinetic energy per site of the band μ . Note that energy of the ground state $|\mathbf{F}\rangle$ is given by

$$E_g = \Lambda \sum_\mu \epsilon_{g\mu} < 0. \quad (3.8)$$

Thus the magnon stiffness constant D_0 is proportional to $|E_g|$:

$$D_0 = \frac{|E_g|}{2S z \Lambda}. \quad (3.9)$$

3.2. Approximation II

It is well known that the RPA overestimates the stability of a ferromagnetic state. To improve upon (3.1), we postulate the state²⁶⁾

$$|\Psi_q\rangle = \Lambda^{-1/2} \sum_i e^{iqr_i} S_i^- |i\rangle, \quad (3.10)$$

where

$$|i\rangle = \Lambda^{-1/2} \sum_{j,\mu} (f_\mu^+(r_j - r_i) c_{i\mu}^\dagger c_{j\mu} + f_\mu^-(r_j - r_i) c_{i\mu} c_{j\mu}^\dagger) |\mathbf{F}\rangle, \quad (3.11)$$

where we expressed $c_{i\mu\uparrow}$ simply as $c_{i\mu}$. The state Ψ_q is constructed so as not to suffer any energy loss by U nor J . Therefore it is used as a trial state for the case $U = J = \infty$. The functions $f_\mu^\pm(r_j - r_i)$ are determined variationally. Note that (3.1) is recovered by assuming $f_\mu^\pm(r_j - r_i) = \delta_{r_j - r_i}$.

We introduce the magnon creation operator S_q^\dagger defined by

$$\Psi_q \equiv S_q^\dagger |F\rangle. \quad (3.12)$$

Then the energy of the variational state (3.10) is given by

$$\omega_q = \frac{\langle F | S_q [H, S_q^\dagger] | F \rangle}{\langle F | S_q S_q^\dagger | F \rangle}. \quad (3.13)$$

After some calculations, we obtain

$$\langle F | S_q S_q^\dagger | F \rangle = \frac{1}{\Lambda} \sum_{k\mu} \Delta_{k\mu}^0 f_{k\mu}^* f_{k\mu} + \frac{1}{\Lambda^2} \sum_{k,p,\mu} \Gamma_{kp\mu}^0 f_{k\mu}^* f_{p\mu}, \quad (3.14)$$

$$\langle F | S_q [H, S_q^\dagger] | F \rangle = \frac{1}{\Lambda} \sum_{k,\mu} \Delta_{kq\mu} f_{k\mu}^* f_{k\mu} + \frac{1}{\Lambda^2} \sum_{k,p,\mu} \Gamma_{kpq\mu} f_{k\mu}^* f_{p\mu}, \quad (3.15)$$

where $f_k = n_k f_k + (1 - n_k) f_k \equiv f_k^+ + f_k^-$ is a sum of the Fourier transform of $f_\mu^\pm(r_j - r_i)$. Quantities appearing in the above expressions are calculated as follows;

$$\Delta_{k\mu}^0 = (2S - n_\mu) n_\mu (1 - n_{k\mu}) + (2S - n_\mu + 1) (1 - n_\mu) n_{k\mu}, \quad (3.16)$$

$$\Gamma_{kp\mu}^0 = (2S - n_\mu) (1 - n_{k\mu}) (1 - n_{p\mu}) + (2S - n_\mu + 1) n_{k\mu} n_{p\mu}, \quad (3.17)$$

$$\begin{aligned} \Delta_{kq\mu} &= (2S - n_\mu) \left(n_\mu \varepsilon_{k\mu} - \frac{1}{\Lambda} \sum_{k'} n_{k'\mu} \varepsilon_{k'\mu} \right) (1 - n_{k\mu}) \\ &+ (2S - n_\mu + 1) \left(\frac{1}{\Lambda} \sum_{k'} (1 - n_{k'\mu}) \varepsilon_{k'\mu} - (1 - n_\mu) \varepsilon_{k\mu} \right) n_{k\mu} \\ &+ \left((1 - n_\mu)^2 \varepsilon_{k+q\mu} - \frac{1}{\Lambda^2} \sum_{k',k''} n_{k'\mu} n_{k''\mu} \varepsilon_{k'-k''-k-q\mu} \right) n_{k\mu}, \end{aligned} \quad (3.18)$$

$$\begin{aligned} \Gamma_{kpq\mu} &= 2(2S - n_\mu) \varepsilon_{k\mu} (n_{k\mu} (1 - n_{p\mu}) - (1 - n_{k\mu}) n_{p\mu}) \\ &+ \left(\frac{1}{\Lambda} \sum_{k'} n_{k'\mu} (\varepsilon_{k'+q\mu} + \varepsilon_{k'-k-p-q\mu}) + (1 - n_\mu) (\varepsilon_{p+q\mu} + \varepsilon_{k+q\mu}) \right) n_{k\mu} n_{p\mu}. \end{aligned} \quad (3.19)$$

If we assume $t_{ij}^\mu = t_\mu$ for the nearest-neighbor pair i, j , $\Delta_{kq\mu}$ and $\Gamma_{kpq\mu}$ are expressed in terms of $\varepsilon_{g\mu}$, (3.7), as

$$\begin{aligned} \Delta_{kq\mu} &= (2S - n_\mu) (n_\mu \varepsilon_{k\mu} + |\varepsilon_{g\mu}|) (1 - n_{k\mu}) \\ &+ (2S - n_\mu + 1) (|\varepsilon_{g\mu}| - (1 - n_\mu) \varepsilon_{k\mu}) n_{k\mu} \\ &+ \left((1 - n_\mu)^2 - \left(\frac{\varepsilon_{g\mu}}{z t_\mu} \right)^2 \right) \varepsilon_{k+q\mu} n_{k\mu}, \end{aligned} \quad (3.20)$$

$$\begin{aligned} \Gamma_{kpq\mu} = & 2(2S - n_\mu)\varepsilon_{k\mu} \left(n_{k\mu}(1 - n_{p\mu}) - (1 - n_{k\mu})n_{p\mu} \right) \\ & + \left(\frac{|\varepsilon_{g\mu}|}{zt_\mu} (\varepsilon_{q\mu} + \varepsilon_{k+p+q\mu}) + (1 - n_\mu)(\varepsilon_{p+q\mu} + \varepsilon_{k+q\mu}) \right) n_{k\mu}n_{p\mu}. \end{aligned} \quad (3.21)$$

These are generalization of our previous results for the ferromagnetic Kondo lattice model.²⁶⁾ Their correspondence becomes clear by introducing the 'localized-spin' S_f ,

$$2S_f \equiv 2S - n_\mu. \quad (3.22)$$

The quantity S_f represents the total spin corresponding to all bands other than that containing the particle under consideration, i.e., all bands except for μ . Generally, S_f depends on the band index μ and can take an arbitrary value, although it must be a half integer in the ferromagnetic Kondo lattice model.²⁶⁾ We use this parameter S_f in the following sections. As noted previously,²⁶⁾ the case $S_f = 0$ can be used to investigate the $U = \infty$ Hubbard model.

We can estimate the spin-wave stiffness D analytically from (3.13).²⁶⁾ The result is

$$\begin{aligned} \omega_q &\equiv Dq^2 \quad (q \rightarrow 0) \\ &= \sum_{\mu} (D_{0\mu} - \Delta D_{\mu})q^2, \end{aligned} \quad (3.23)$$

where $D_{0\mu}$ is defined in (3.6), and

$$\Delta D_{\mu} = \frac{1}{2S} \frac{(1 - n_\mu)^2 I_{\mu}}{1 + (|\varepsilon_{g\mu}|/zt_\mu)(I_{\mu}/2t_\mu)}, \quad (> 0) \quad (3.24)$$

$$I_{\mu} = \frac{1}{\Lambda} \sum_k \frac{v_{k\mu}^2}{\Delta_{k0\mu}} n_{k\mu}, \quad (3.25)$$

$$v_{k\mu} = \frac{\partial \varepsilon_{k\mu}}{\partial k}. \quad (3.26)$$

These expressions for D , below (3.23), will be used in the following sections.

§4. Individual-particle excitation

To describe the individual-particle excitation which has a spin component antiparallel to the spontaneous magnetization, we introduce the following creation operator for the quasiparticle in the band μ :

$$C_{k\mu\downarrow}^\dagger = \frac{1}{\Lambda} \sum_{i,j} e^{ikr_i} \left(h_U c_{i\mu\downarrow}^\dagger + \sum_{\nu} h_{j-i\mu}^\nu s_{i\nu}^- c_{j\mu}^\dagger \right). \quad (4.1)$$

The expression (4.1) for $h_U = 0$ and $h_{j-i\mu}^\nu = \delta_{ij}$ appears as a prefactor of $c_{j\mu}$ in Ψ_q . In this case, the trial state does not suffer energy loss due to U nor J . To include the effect of finite interactions, we introduce a variational parameter h_U and assume

the dependence of $h_{j-i\mu}^\nu$ on $\mu - \nu$. The dependence on $r_j - r_i$ is further assumed to afford a better variational description. This corresponds to allowing an up-spin particle ($c_{j\mu}^\dagger$ in (4.1)) to be created at a site different than the site i where a down-spin particle is created by $s_{i\nu}^-$. As will be seen below, the effect of multiple magnon scattering is taken into account by this generalization.

The energy expectation value of (4.1) is given by

$$E_{k\mu\downarrow} = \frac{\langle \mathbf{F} | C_{k\mu\downarrow} [H, C_{k\mu\downarrow}^\dagger] | \mathbf{F} \rangle}{\langle \mathbf{F} | C_{k\mu\downarrow} C_{k\mu\downarrow}^\dagger | \mathbf{F} \rangle}, \quad (4.2)$$

for which we obtain

$$\begin{aligned} \langle \mathbf{F} | C_{k\mu\downarrow} C_{k\mu\downarrow}^\dagger | \mathbf{F} \rangle &= \frac{1}{\Lambda} \sum_{k_1, \nu} n_\nu |h_{k_1\mu}^\nu|^2 + \left| h_U + \frac{1}{\Lambda} \sum_{k_1} h_{k_1\mu}^\mu \right|^2, \quad (4.3) \\ \langle \mathbf{F} | C_{k\mu\downarrow} [H, C_{k\mu\downarrow}^\dagger] | \mathbf{F} \rangle &= \frac{1}{\Lambda} \sum_{k_1, \nu} |h_{k_1\mu}^\nu|^2 \left(n_\nu \varepsilon_{k_1\mu} + \frac{1}{\Lambda} \sum_{k_2} n_{k_2\nu} (\varepsilon_{k-k_1+k_2\nu} - \varepsilon_{k_2\nu}) \right) \\ &\quad + \left| h_U + \frac{1}{\Lambda} \sum_{k_1} h_{k_1\mu}^\mu \right|^2 \varepsilon_{k\mu} + g_\mu |h_U|^2 \\ &\quad + \frac{J}{2} \sum_{\nu(\neq\mu)} n_\nu \left(n_\mu \sum_{k_1} |h_{k_1\mu}^\mu - h_{k_1\mu}^\nu|^2 + \left| \sum_{k_1} (h_{k_1\mu}^\mu - h_{k_1\mu}^\nu) \right|^2 \right), \quad (4.4) \end{aligned}$$

where $h_{k\mu}^\nu$ is the Fourier transform of $h_{i\mu}^\nu$ multiplied by $1 - n_{k\mu}$. The parameter g_μ is defined by

$$g_\mu \equiv U n_\mu + J S_f, \quad (4.5)$$

and represents the Hartree-Fock exchange splitting of our model.

We remark that we must assume (i) $h_U = 0$ for $U = \infty$, and (ii) $h_{k_1\mu}^\nu = h_{k_1\mu}^\mu$ and $h_U = 0$ for $J = \infty$, as noted above. This is because the terms depending on g_μ and/or J in (4.4), which are positive definite, should vanish in the strong coupling limit.

4.1. Case $J \neq \infty$

As the above expressions are too general and complicated, we show simpler expressions which are used in the following investigation. To investigate the effect of a finite Hund's-rule coupling J , we introduce a new variational parameter h_J by

$$h_{k\mu}^\nu = h_J h_{k\mu}^\mu. \quad (4.6)$$

The parameter h_J measures the effect of the Hund's-rule coupling. In particular, $h_J = 0$ for $J = 0$, and $h_J = 1$ for $J = \infty$.

All terms but the last term of (4.4) are independent of the phase of the complex quantity h_J . Therefore, it is always energetically unfavorable to have $h_{k_1\mu}^\nu$ out of

phase with $h_{k_1\mu}^\mu$. Thus, we may assume h_J as a real quantity, $0 \leq h_{k_1\mu}^\nu \leq 1$. This implies that the spins $\mathbf{s}_{i\mu}$ at site i should couple in phase with each other by the Hund's-rule coupling. For $h_J = 1$, the spin lowering operator $\sum_\nu h_{j-i\mu}^\nu s_{i\nu}^-$ in (4.1) reduces to a quantity proportional to (3.2).

After taking the functional derivative of (4.2) with respect to h_U and $h_{k_1\mu}^\mu$ and eliminating these parameters, one obtains the eigenequation for the excitation energy $E_{k\mu\downarrow}$,²⁶⁾

$$E_{k\mu\downarrow} - \varepsilon_{k\mu} = \Sigma_\mu(k, E_{k\mu\downarrow}), \quad (4.7)$$

$$\Sigma_\mu(k, E_{k\mu\downarrow}) = \frac{g_\mu(1 - j_\mu\tilde{\rho})}{1 - (g_\mu + j_\mu)\tilde{\rho}}, \quad (4.8)$$

where

$$\tilde{\rho} \equiv \frac{1}{\Lambda} \sum_{k_1} \frac{1 - n_{k_1\mu}}{(2S_f h_J + n_\mu)(E_{k\mu\downarrow} - \omega'_{\mu k-k_1} - \varepsilon_{k_1\mu}) - n_\mu j_\mu}, \quad (4.9)$$

$$\omega'_{\mu q} \equiv \frac{1}{2S_f h_J + n_\mu} \frac{1}{\Lambda} \sum_{k_2, \nu} (h_J + (1 - h_J)\delta_{\mu\nu}) n_{k_2\nu} (\varepsilon_{q+k_2\nu} - \varepsilon_{k_2\nu}), \quad (4.10)$$

and

$$j_\mu \equiv JS_f(1 - h_J)^2. \quad (4.11)$$

Noting the identity

$$\frac{1}{\Lambda} \sum_{k_2, \nu} n_{k_2\nu} (h_J + (1 - h_J)\delta_{\mu\nu}) = 2S_f h_J + n_\mu, \quad (4.12)$$

and comparing $\omega'_{\mu q}$ with (3.3), we observe that $\omega'_{\mu q}$ is the generalization of the magnon dispersion in the presence of the inter-band spin-spin coupling. For the complete coupling $h_J = 1$, (3.3) is recovered, while $h_J = 0$ gives the single-band result for the band μ .

Since further variation with respect to h_J leads to a complicated expression, we leave h_J as a parameter. Thus, the equation (4.7) is to be solved for $E_{k\mu\downarrow}$ as a function of h_J , which in turn should be determined so as to minimize $E_{k\mu\downarrow}$. The expressions following (4.7) are conclusions of this subsection. We note that the derivation of (4.7) from (4.1) is exact. While an assumption is made in (4.6), this does not conflict with the variational principle. Introduction of the single parameter h_J to describe the Hund's-rule coupling is largely for the sake of simplicity.

4.2. Case $h_J = 1$

The case $h_J = 1$ is realized for $J = \infty$, where the Hubbard repulsion U is always ineffective. This is because the strong Hund's-rule coupling forbids two particles to stay on the same site. However, there is a situation in which the assumption $h_J = 1$ and $h_U \neq 0$ is adequate even for a finite interaction $J < \infty$. We observed that this is in fact the case for the double exchange ferromagnet.²⁶⁾ By this assumption, the number of variational parameters decreases by one, and the calculation becomes relatively easy.

In this case, from the results of the previous subsection, we obtain an eigenequation of the form

$$E_{k\mu\downarrow} - \varepsilon_{k\mu} - \Sigma_\mu(k, E_{k\mu\downarrow}) = 0, \quad (4.13)$$

where

$$\Sigma_\mu(k, \omega) = \frac{g_\mu}{1 - \Sigma_\mu^0(k, \omega)/g_\mu}, \quad (4.14)$$

and

$$\Sigma_\mu^0(k, \omega) = \frac{g_\mu^2}{2S} \frac{1}{\Lambda} \sum_{k_1} \frac{1 - n_{k_1\mu}}{\omega - \omega_{0k-k_1} - \varepsilon_{k_1\mu}}. \quad (4.15)$$

The magnon energy ω_{0q} is defined in (3.3).

In these forms, it is possible to regard $\Sigma_\mu(k, \omega)$ as the self-energy given as a result of the multiple scattering of quasiparticle $\varepsilon_{k_1\mu}$ off the spin wave ω_{0k-k_1} . In fact, a particular case of this result, for the single-band Hubbard model $2S = n$ and $g = Un$, has already been obtained by many authors.^{17), 19), 20), 21), 23)} Although the formulae we derived have the same forms as those derived in the other methods, it contains a meaning more significant than that of mere re-derivation. Since our results are based on the variational principle, we can draw a definite conclusion on the instability of the ferromagnetic state.

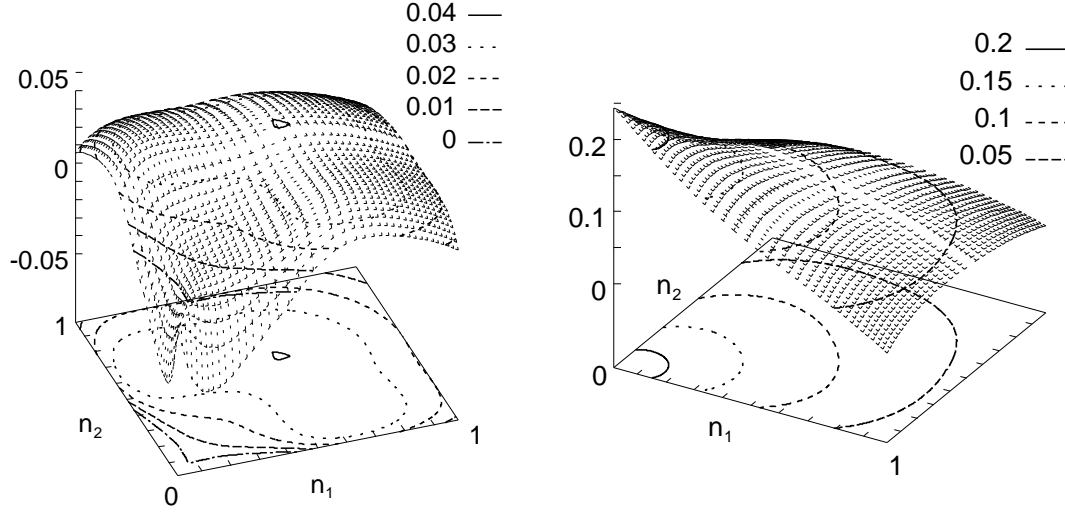
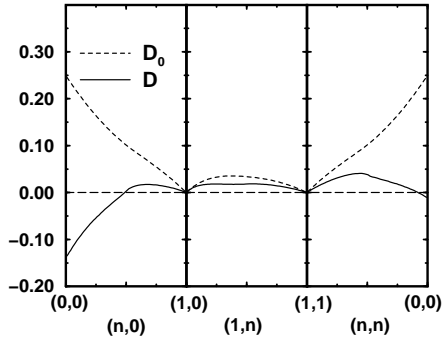
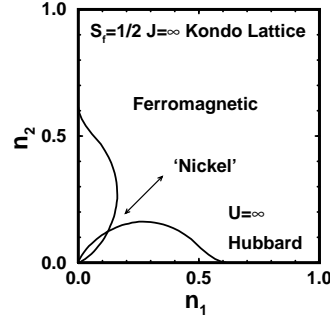
§5. Two-band model

In this section we consider a simple case to show general features of our model. We investigate a special case of (2.12), i.e., a model comprising two bands in a tight-binding square lattice structure. Then the band dispersion is given by $\varepsilon_{k\mu} = -2t(\cos(k_x) + \cos(k_y))$ ($\mu = 1, 2, t > 0$), and the band-width is $2zt$ with $z = 4$. This model includes the Hubbard model and the $S_f = 1/2$ ferromagnetic Kondo lattice model as special cases. Therefore we can treat them in a unified way. Parameters used in the following discussion are the interaction U, J , and the carrier density n_μ of the band μ . The purpose of this section is to investigate the effect of the orbital degeneracy and the Hund's-rule coupling.

5.1. Spin wave

In this and the next subsection, we consider the strong coupling limit $U = J = \infty$, where the formulae given in §3 are of direct use. In Fig. 1, we show the spin-wave stiffness constant $D(n_1, n_2)$ as well as $D_0(n_1, n_2)$ as a function of n_1 and n_2 , where D_0 is given by (3.9) and D is defined below (3.23). In Fig. 2, they are shown along the symmetry axes in the n_1 - n_2 plane.

If the effect of band degeneracy is simply additive, one should expect $D(n, n) = D(n, 0) = D(0, n)$. In fact, this holds for the result D_0 in the RPA, for which the curve determined by $D_0(n_1, n_2) = \text{const}$ becomes convex in the direction $(n_1, n_2) = (1, 1)$ (Fig. 1). However, this is not the case for the improved estimate $D(n_1, n_2)$; the curve $D(n_1, n_2) = 0$ is concave instead, as shown in the dash-dotted contour line on the left of Fig. 1. This is due to a singularity present in $D(n_1, n_2)$ at $(n_1, n_2) = (0, 0)$. Here we note that $D(n_1, n_2) = 0$ defines the threshold for ferromagnetism. In our


 Fig. 1. Spin-wave stiffness constant $D(n_1, n_2)$ (left) and $D_0(n_1, n_2)$ (right).

 Fig. 2. Spin-wave stiffness constant D and D_0 as a function of (n_1, n_2) .

 Fig. 3. Phase boundary determined by the condition $E_{k1\downarrow} = \varepsilon_f$ and $E_{k2\downarrow} = \varepsilon_f$ with $k = 0$. In the region enclosed by the curves, the ferromagnetic state is absolutely unstable.

treatment, the result $D < 0$ represents the absolute instability of the ferromagnetic state. From the displayed results, we understand that a multi-band model favors ferromagnetism more than a single-band model and that one should go beyond the RPA to show this multi-band effect. In the RPA, we cannot prove instability at all, since $D_0 > 0$ for any (n_1, n_2) (see Fig. 2). In particular, one should be careful in treating the low-density limit owing to the presence of the singularity mentioned above. This point is discussed later.

Next, we note that the line along $(n, 0)$ or $(0, n)$ ($0 \leq n \leq 1$) corresponds to the $U = \infty$ Hubbard model and the line along $(n, 1)$ or $(1, n)$ to the ferromagnetic Kondo lattice model with $S_f = 1/2$ and $J = \infty$. These two cases were discussed in

Ref. 26). As a new result, in the direction (n, n) , i.e., in the case $n_1 = n_2$, the singular behavior around $(0,0)$ makes the threshold value so small as $n_c \lesssim 0.1$. (See D in Figs. 1 and 2). We note that the ferromagnetic state is unstable for $n < n_c$, while we may assume $n_{\text{Ni}} \sim 0.2$ for Ni. Thus one may simply consider that the fact $n_{\text{Ni}} > n_c$ is relevant to the itinerant ferromagnetism in Ni. This point is addressed in the next subsection, since the more stringent condition is obtained by investigating the individual-particle excitation.

5.2. Individual-particle excitation

On the stability of the ferromagnetic state, investigation of the individual-particle excitation produces a more stringent condition than that given by the spin-wave stiffness constant.²⁶⁾ To investigate the case $U = J = \infty$, we use the expressions given in §4.2. The eigenenergy $E_{k\mu\downarrow}$, regarded as a real quantity, is calculated as a solution of (4.13) \sim (4.15). We determined the critical boundary in the n_1 - n_2 plane using the condition $E_{k\mu\downarrow} = \varepsilon_{f\mu}$ ($\mu = 1, 2$), where we set $k = 0$ for the bottom of the dispersion $\varepsilon_{k\mu}$. The result is shown in Fig. 3. The Fermi energy $\varepsilon_{f\mu}$ is fixed for a given n_μ . The ferromagnetic state is absolutely unstable when $E_{k\mu\downarrow} < \varepsilon_{f\mu}$.

As mentioned, threshold curves thus obtained give a more stringent condition than that determined by the relation $D(n_1, n_2) = 0$. (Compare Fig. 3 with the contour line $D = 0$ of Fig. 1.) In particular, in the direction (n, n) , the critical concentration is estimated as $n_c \sim 0.12$. In this respect, let us remark again that the stiffness D has a singularity, as noted in the previous subsection. This is due to the denominator $2S \rightarrow 0$ as $n \rightarrow 0$ in the expression for the stiffness constant D , (3.24). On the other hand, $D_0(n_1, n_2)$ goes to a finite value in this limit $(n_1, n_2) \rightarrow (0, 0)$ (Fig. 2), because the numerator of (3.9) also vanishes in this limit. Thus, the correction $\Delta D/D_0$ is largest in the vicinity of the origin, as seen in Figs. 1 and 2. On the other side, the equation (4.13) for $E_{k\mu\downarrow}$ contains the spin-wave energy $\omega_0(q)$ in the denominator of $\Sigma_\mu^0(k, \omega)$, (4.15). Our calculation based on (4.1) is exact, so that our result gives the exact lower bound for n_c . Nonetheless, in a physical (i.e. non-rigorous) sense for improving the approximation, one should replace $\omega_0(q) \simeq D_0 q^2$ in (4.15) with $\omega(q) \simeq D q^2$. In this replacement, a more stringent and realistic condition will be obtained, although it then loses variational significance.²⁶⁾ As a result, we expect that the critical boundary in the region where $D \ll D_0$ is drastically modified as the approximation is improved. For example, from Fig. 2 along the line $(1, n)$, i.e., for the double exchange ferromagnet with $S_f=1/2$, the correction will be less prominent than the case along $(n, 0)$, the $U=\infty$ Hubbard model. Around the origin, D differs considerably from D_0 (Figs. 1 and 2), so that the critical n_c in a proper treatment will take a larger value than $n_c \sim 0.12$ of Fig. 3. However, it is still legitimate to assert that the doubly-degenerate-band model is more favorable to ferromagnetism than the single-band model, although in the following section we stress that ferromagnetism of Ni cannot be explained only by the effect of orbital degeneracy, but a peculiarity of the density of states is required in addition (§6).

In any case, we note that the correction $\Delta D/D_0$ (3.24) is a quantity of order $\sim O(1/S)$ for large S , since $\Delta_{k0\mu}$ in I_μ (3.25) is proportional to S . Therefore, the RPA is quite reliable for models with highly degenerate orbitals and/or a large

spontaneous magnetization, as is expected intuitively.

5.3. The effect of the Hund's-rule coupling

In this subsection, we assume U to be infinite but J to be finite in order to consider the effect of the Hund's-rule coupling. As in the above subsections, the model consists of the two Hubbard models in the square lattice, coupled to each other by the Hund's-rule coupling.

We are interested in the effect of the interaction J which couples the two bands. Previously it was concluded that the ferromagnetic state in the single-band Hubbard model (the limit $J \rightarrow 0$ of the present model) is unstable beyond some critical hole concentration $\delta_c \equiv 1 - n_c$, while it is stable for an arbitrary concentration in the $S_f=1/2$ Kondo lattice model (the limit $J \rightarrow \infty$). On the other hand, as we saw in the previous subsections, the model which assumes $n_1 = n_2$ is more stable than the single-band model, although it would be less stable than the double exchange ferromagnet with $S_f=1/2$. To interpolate these situations in terms of J , the critical carrier density determined by the quasiparticle energy is given below as a function of J . To this end, we use the formulae given in §4.1.

The eigenenergy $E_{k\mu\downarrow}$ is obtained as a solution of (4.7) with

$$\Sigma_\mu(k, E_{k\mu\downarrow}) = j_\mu - \frac{1}{\tilde{\rho}}, \quad (5.1)$$

since $g_\mu = \infty$ for $U = \infty$. Here, $\tilde{\rho}$ and j_μ are functions of h_J and n_μ (or S_f), and are defined in (4.9) and (4.11), respectively. As noted there, the variational parameter h_J has been left as a parameter to be determined to minimize the energy. However, in determining the phase boundary, minimization on h_J is not necessary; we only have to calculate J to satisfy $E_{k\mu\downarrow} = \varepsilon_f$ for a fixed carrier density n and for various values of h_J . The envelope formed by a set of curves for every h_J then gives the threshold J as a function of n , since the variational principle implies instability in all cases if it is the case for any of h_J .

We give results for the model (i) for which we set $n_1 = 1$ and $n_2 = n$ (Fig. 4), and for the model (ii) with $n_1 = n_2 = n$ (Fig. 5). In the former, the single-band Hubbard model is interpolated to the $S_f=1/2$ ferromagnetic Kondo lattice model. In the latter, it is interpolated as a function of J to the case of two equivalent Hubbard models strongly coupled via Hund's rule.

For the model (i) (see Fig. 4) the region in which the ferromagnetic state is stable is quite large. In particular, the Hund's-rule coupling becomes effective even for J as small as $0.5zt$, a quarter of the band-width $W = 2zt$. For large J the ferromagnetic phase becomes stable for arbitrary n , as expected for the double exchange model. The critical boundary (envelope, thick curve) in Fig. 4 is determined by curves for relatively small values $h_J \lesssim 0.4$, as expected for the boundary in the weak-coupling region; curves with larger h_J are completely surrounded by the envelope and do not contribute to it.

For the model (ii) (see Fig. 5) the envelope strongly bends upward around $J \sim 2zt \equiv W$. This implies that the Hund's-rule coupling becomes effective when the coupling energy becomes comparable with the band width. The critical hole

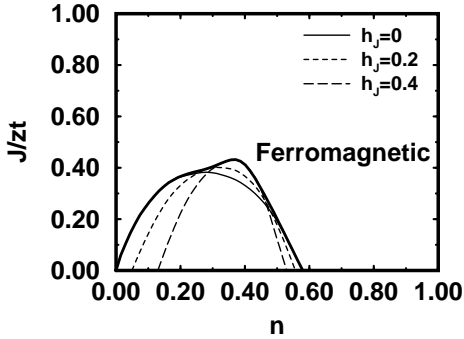


Fig. 4. Thick line: Threshold for the stability of the ferromagnetic state. The model consists of the $U = \infty$ Hubbard model and an array of localized spins $S_f = 1/2$ coupled to each other by J .

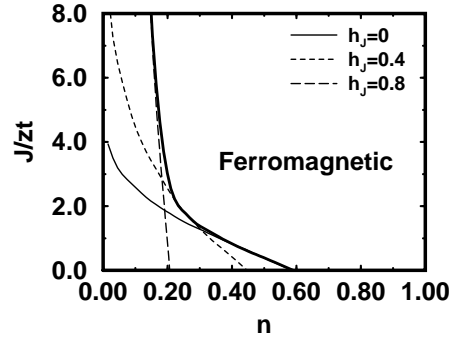


Fig. 5. Thick line: Threshold for the stability of the ferromagnetic state. The model consists of two equivalent $U = \infty$ Hubbard models coupled by J .

concentration δ_c increases from $\delta_c \sim 0.4$ for the $U=\infty$ Hubbard model to $\delta_c \sim 0.9$ as J increases from zero to infinity. This, and especially a steep increase in δ_c around $J \sim 0$ clearly indicate the importance of the inter-band spin-spin coupling. Thus it is concluded that the stability condition based on a single-band model becomes more stringent than what should be obtained for realistic bands with orbital degeneracy. The Hund's-rule coupling effect, if not complete (or even if $h_J \neq 1$), can change the criterion for the ferromagnetic instability to a degree that it cannot be neglected in investigating real materials. In the next section, we discuss the itinerant ferromagnetism in Ni, where the importance of the Hund's-rule coupling is again stressed.

§6. Ferromagnetism in nickel metal

Discussion given above has been based on the expressions derived variationally in §§3 and 4. Thus the results indicating instability of the ferromagnetic state are exact. However, in discussing itinerant ferromagnetism of metallic nickel, we prefer to give a physical argument since a model for Ni has to be simple enough to be tractable. A model density-of-states that we adopt below has some characteristic features which are regarded to be relevant to ferromagnetism in Ni. We do not attempt to estimate the magnon dispersion, for example, by using our expression for D , since we are not sure that the model given below is so quantitative as to reproduce an appropriate estimate even for the spin wave spectrum. Therefore, we regard the spin-wave stiffness constant D as a given quantity and substitute the dispersion $\omega_q = Dq^2$ for ω'_q in (4.9). The model and parameters used below are set so as to mimic metallic nickel.

6.1. Simple model simulating Ni

To describe metallic nickel, we adopt a simple model as a matter of convenience. As one of important characteristic, the density of states of Ni at the Fermi level ρ_f takes a quite large value. This is doubtless an important factor for ferromagnetism, as indicated from the Stoner criterion $\rho_f U > 1$. Thus, as an example of models simulating Ni, we adopt the model due to Edwards and Hertz,²¹⁾ i.e., with the isotropic dispersion ε_k depending on k quadratically:

$$\varepsilon_k = \begin{cases} \frac{k^2}{2m_1} & , \quad 0 \leq k \leq k_1, \\ \frac{k^2}{2m_2} - C & , \quad k_1 \leq k \leq k_D. \end{cases} \quad (6.1)$$

Here, the constant C is chosen to make ε_k continuous at k_1 . The quantity $k_D = (6\pi^2)^{1/3}$ is a Debye-like cutoff chosen so that the band contains one electron state per spin per orbital. The parameters m_1 and m_2 are determined so as to meet the following conditions. (i) For the Fermi wave-vector $k_f = k_1$, the total density per band is $n = 0.2$. (ii) The bandwidth is 4 eV. For the Fermi energy, we introduce a parameter $\varepsilon_1 (\equiv \varepsilon_{k_1})$ which characterizes a peculiarity of the density of states. The parameter k_1 in (6.1) is uniquely determined by the condition (i). Then, m_1 is set by $\varepsilon_{k_1} = \varepsilon_1$ for a given ε_1 . Parameters m_2 and C are determined to give the total band width 4 eV and $\varepsilon_{k_1-0} = \varepsilon_{k_1+0}$. If we assume $\varepsilon_1 = 0.3$ eV to mimic Ni, then $m_1 = 8.66$ and $m_2 = 1.35$.²¹⁾ These choices are based on the hole picture¹⁾ in which 0.6 d -hole per nickel atom occupies three sub-bands. Moreover we assume the quadratic dispersion for the magnon,²¹⁾

$$\omega'_q = Dq^2, \quad (6.2)$$

where the stiffness constant is set such that $Dk_1^2 = 0.2$ eV. The density of states for the model (6.1) is shown in Fig. 6.

We investigate a model consisting of three equivalent sub-bands, each of which has the dispersion ε_k as given above. The Hund's-rule coupling J increases the mean-field exchange splitting g defined in (4.5). This effect, however, is due to the longitudinal component of the coupling. Therefore, to investigate the transverse coupling effect, which has been discussed only little, we take g (or g/n) as a parameter for the one-particle bare interaction energy. Thus, for given g/n , J and n , a set of equations (4.7) ~ (4.9) are solved for $E_{k\mu\downarrow}$. Results for a single-band model are obtained by setting $J = 0$ and $h_J = 0$. Note that the parameter $\bar{U} \equiv g/n$ represents $\bar{U} = U$ for the single-band model and $\bar{U} = U + J$ for the model with triply-degenerate orbitals. The parameters used below are g/n , n , J and ε_1 .

6.2. Results

First, we show the phase boundary determined by $E_{k=0\mu\downarrow} = \varepsilon_f$ for the degenerate-band model, as well as that of the single-band model (the case $J = 0$ and $h_J = 0$). The critical interaction $\bar{U}_c \equiv g_c/n$ (eV) as a function of the carrier density n is shown in Fig. 7 for $\varepsilon_1 = 0.3$ eV. Since we should have $g/n \lesssim 4$ eV and $n = 0.2$ for

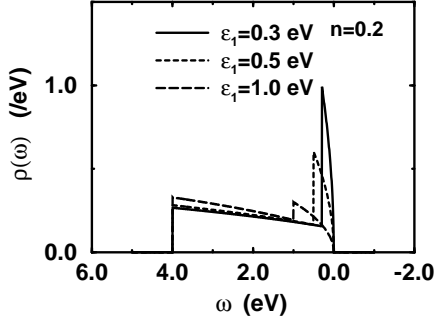


Fig. 6. Bare density of states of our model for metallic nickel. In the ferromagnetic state, a carrier of total density $n = 0.2$ per band occupies up to the Fermi energy ε_1 (eV).

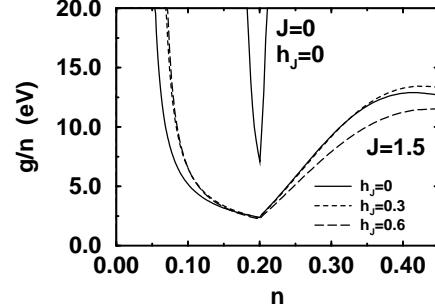


Fig. 7. The critical value of g/n as a function of n for $\varepsilon_1 = 0.3$ eV. In the region below the curve, the complete ferromagnetic state is unstable. The curve for $J = 0$ and $h_J = 0$ represents the result for the single-band model.

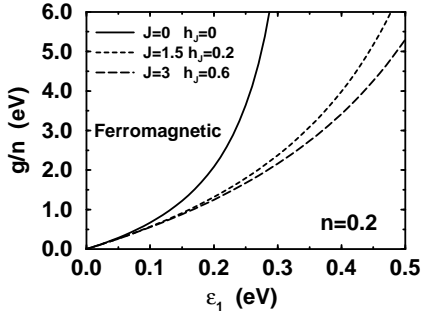


Fig. 8. The critical value of g/n as a function of ε_1 for $n = 0.2$. In the region below the curve, the complete ferromagnetic state is absolutely unstable. The parameters h_J shown for $J = 1.5$ and $J = 3$ are those which give the most stringent criterion.

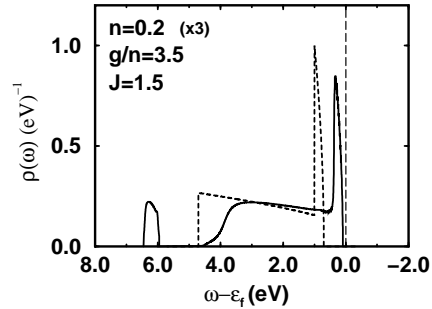


Fig. 9. Density of states $\rho(\omega)$ for $g/n = 3.5$, $J = 1.5$, and $h_J = 0.2$. The carrier density is $n = 0.2$ for each of triply-degenerate bands. The dashed curve represents the Hartree-Fock result. The Fermi energy is $\varepsilon_f = \varepsilon_1 = 0.3$ eV.

Ni, we conclude that the Hund's-rule coupling is necessary to stabilize the ferromagnetic ground state. Here we give some examples of the results: For $n = 0.2$ and $g/n = 4$ eV, the ferromagnetic state becomes unstable for $J \lesssim 0.3$ eV, and h_J becomes non-zero for $J \gtrsim 1.3$ eV, while $h_J = 0.7$ for $J = 3$ eV.

After the importance of the the Hund's-rule coupling is shown, the next question is that concerning a peculiarity in the bare density of states. We know that a large density of states is not necessary for ferromagnetism in the ferromagnetic Kondo lattice model. However, in metallic Ni, the carrier density is so low that it is not

clear if the Hund's-rule coupling alone can stabilize the ferromagnetic state. To see the effect, one may change the parameter ε_1 , which is set above as 0.3 eV. We display the phase boundary g/n as a function of ε_1 for $n = 0.2$ (Fig. 8). Note that states of total weight $n = 0.2$ occupy up to ε_1 (eV) within the band of 4 eV wide. Thus a small ε_1 represents a strong peculiarity, favoring ferromagnetism. (See Fig. 6.) We see in Fig. 8 that the Hund's-rule coupling is necessary to keep the relevant region around $(\varepsilon_1, g/n) \simeq (0.3, 4.0)$ eV ferromagnetic. Still, a large bare density-of-states is also required, as concluded in Ref. 25). Note that we require ε_1 to be as large as $4(k_1/k_D)^2 = 1.37$ eV to give a simple parabolic band, for which $m_1 = m_2$. Even with $\varepsilon_1 \sim 0.5$ eV, the peak structure in the density of states is pronounced, as shown in Fig. 6.

Although the phase boundary in Fig. 7 around $n \simeq 0.2$ does not depend strongly on h_J , the coupling in terms of h_J plays an important role. This point is clearly seen in the renormalized density-of-states curve $\rho(\omega)$. To investigate whether we obtain the satellite structure, we calculate $\rho(\omega)$ defined by

$$\rho(\omega) \equiv -\frac{1}{\pi} \text{Im} \frac{1}{A} \sum_k \frac{1}{\omega - (\varepsilon_k - \varepsilon_f) - \Sigma(k, \omega)}, \quad (6.3)$$

where $\Sigma(k, \omega)$ is given by (4.8). In order to estimate the position of a satellite structure, one may neglect the momentum dependence of $\Sigma(k, \omega)$, or ω_q may be replaced with the quantity averaged over q : $\bar{\omega}_q \equiv \frac{3}{5} D k_D^2$.²⁶⁾ Then, the calculation is straightforward, and the result is shown in Fig. 9 for $\varepsilon_1 = 0.3$ eV.

It is important to note that we can assume parameters so as to reproduce the 6 eV satellite structure while preventing the instability of the ferromagnetic state. In the figure, we set $g/n = 3.5$ eV, $J = 1.5$ eV and $n = 0.2$. The parameter $h_J = 0.2$ is determined to minimize $E_{k=0\mu\downarrow}$. These values for g/n and J are physically reasonable for metallic nickel. In the calculation with the other set of parameters, we observed that the position of the satellite depends on h_J , if it is regarded formally as a free parameter. For example, for the same set of parameters except for h_J , the satellite appears at 5 eV and 7.7 eV for $h_J = 0$ and 1, respectively. The weight of the satellite also depends on h_J and is an increasing function of h_J . This is physically interpreted as follows: The weight in the low-lying part of spectrum (the part other than that due to the satellite) decreases as the local constraint from the coupling J becomes effective, or as h_J increases.²⁶⁾

§7. Conclusion

We investigated the effect of the Hund's-rule coupling and the orbital degeneracy on the basis of the variational treatment of a general model for the itinerant ferromagnet. Our model includes the ferromagnetic Kondo lattice model and the Hubbard model as special cases. It was also applied to the ferromagnetism in Ni. To investigate instability due to individual particle excitation, we took into account the multiple magnon scattering effect and reproduced some of the results which were derived in the Hubbard model by many authors. Generally, in the theory of itinerant ferromagnetism, it is important to meet the requirement imposed by the

rotational symmetry of the model Hamiltonian. In terms of the diagram technique, one should take into account the vertex correction in accordance with the Ward-Takahashi identity.^{18), 20), 31)} In this respect, we avoided complexity by making use of proper variational states. We derived the required expressions variationally without any ambiguous assumption. Variational derivation is advantageous because we do not have to be concerned with the problem of selecting the type of diagrams to be summed over and we are free from a convergence problem of the summed infinite series. Moreover, the result for the instability has an exact significance, since it follows the variational principle.

We clarified the physics introduced by the Hund's-rule coupling by treating a two-band model and a model simulating metallic nickel. For the former, we noted that attention should be paid to the treatment of the low-density limit of the degenerate-band model, owing to the singular behavior of the spin-wave stiffness constant D . We displayed figures for D which show that the correction to the result of the RPA becomes smaller when the spontaneous magnetization becomes larger. Investigation of the individual-particle excitation gives a more stringent condition for the instability of the ferromagnetic state than that given by the spin-wave instability. However, in both cases, we observed a common tendency that a two-band model is quite stable compared with a single-band model. As a function of the Hund's-rule coupling J , we investigated how two bands are ferromagnetically coupled. In the case where one of them constitutes localized spins, J is quite effective, as expected. In the other case, where the two bands are equivalent, J stabilizes the ferromagnetic state in the regime $J \lesssim W$. We conclude for Ni that a peculiarity of the density-of-state curve at the Fermi level is indispensable, while the effect of Hund's-rule coupling is also required. In this respect, ferromagnetism in Ni differs from the double exchange ferromagnet, in which the complete ferromagnetic state is made stable only by the Hund's rule coupling. However, it is conceptually simple to discuss itinerant ferromagnetism on the basis of a unified model as we proposed in this article. It was also shown that the effect of the Hund's-rule coupling including its transverse component can explain the 6 eV satellite structure as well as the ferromagnetic ground state of metallic nickel.

Acknowledgments

The author would like to thank Professor K. Yamada for discussions and T. Ichinomiya and S. Yoda for their helpful assistance in preparing the manuscript and figures. This work is supported by Research Fellowships of the Japan Society for the Promotion of Science for Young Scientists.

References

- [1] J. Kanamori, Prog. Theor. Phys. **30** (1963), 275.
- [2] M. C. Gutzwiller, Phys. Rev. Lett. **10** (1963), 159.
- [3] J. Hubbard, Proc. R. Soc. London **A276** (1963), 238.
- [4] Y. Nagaoka, Phys. Rev. **147** (1966), 392.
- [5] H. Tasaki, Phys. Rev. Lett. **69** (1992), 1608.
A. Mielke and H. Tasaki, Commun. Math. Phys. **158** (1993), 341.

- [6] K. Penc, H. Shiba, F. Mila and T. Tsukagoshi, Phys. Rev. **B54** (1996), 4056.
- [7] In the strong-coupling regime of the Hubbard model, it is generally more difficult to prove instability of the ferromagnetic state for the density just around half-filling than for low densities. This is concluded at least by a variational treatment, e.g., in Fig. 3 of this article. Although this does not necessarily mean that the ferromagnetic state is actually realized in the single-band Hubbard model, this conclusion is consistent with the result of Nagaoka.³⁰⁾ Therefore, we simply call this hypothetical ferromagnetic state the Nagaoka ferromagnetic state, although the origin of its stability may not be regarded as due to a coherent motion of doped holes, as first envisaged by Nagaoka.
- [8] E. Antonides, E. C. Janse and G. A. Sawatzky, Phys. Rev. **B15** (1977), 1669.
- [9] J. C. Fuggle, P. Bennett, F. U. Hillebrecht, A. Lenselink and G. A. Sawatzky, Phys. Rev. Lett. **49** (1982), 1787.
- [10] P. Bennett, J. C. Fuggle, F. U. Hillebrecht, A. Lenselink and G. A. Sawatzky, Phys. Rev. **B27** (1983), 2194.
- [11] S. Hüfner and G. K. Wertheim, Phys. Lett. **51A** (1975), 299.
- [12] P. C. Kemeny and N. J. Shevchik, Solid State Commun. **17** (1975), 255.
- [13] R. J. Smith, J. Anderson, J. Hermanson and G. J. Lapeyre, Solid State Commun. **21** (1977), 459.
- [14] C. Guillot, Y. Ballu, J. Paigné, J. Lecante, K. P. Jain, P. Thiry, R. Pinchaux, Y. Pétroff and L. M. Falicov, Phys. Rev. Lett. **39** (1977), 1632.
- [15] D. Penn, Phys. Rev. Lett. **42** (1979), 921.
- [16] G. Treglia, F. Ducastelle and D. Spanjaard, J. Physique, **41** (1980), 281.
- [17] D. M. Edwards, J. Appl. Phys. **39** (1968), 481.
- [18] U. Brandt, Z. Phys. **244** (1971), 217.
- [19] L. M. Roth, Phys. Rev. **186** (1969), 428.
- [20] J. A. Hertz and D. M. Edwards, J. of Phys. **F3** (1973), 2174.
- [21] D. M. Edwards and J. A. Hertz, J. of Phys. **F3** (1973), 2191.
- [22] A. Liebsch, Phys. Rev. Lett. **43** (1979), 1431.
- [23] A. Liebsch, Phys. Rev. **B23** (1981), 5203.
- [24] J. Igarashi, *Electron Correlation and Magnetism in Narrow-Band Systems*, ed. T. Moriya (Springer Verlag, 1981), p168.
- [25] T. Okabe, J. Phys. Soc. Jpn. **65** (1994), 1056; **66** (1997), No.7.
- [26] T. Okabe, Prog. Theor. Phys. **97** (1997), 21; **97** (1997), 559.
- [27] V. L. Moruzzi, J. F. Janak and A. R. Williams, *Calculated Electronic Properties of Metals* (Pergamon, 1978).
- [28] In view of experimental results,^{9), 10)} this is not an unreasonable assumption.
- [29] L. M. Roth, J. Phys. Chem. Solids **28** (1967), 1549; J. Appl. Phys. **39** (1968), 474.
- [30] B. S. Shastry, H. R. Krishnamurthy and P. W. Anderson, Phys. Rev. **B41** (1990), 2375.
- [31] H. Matsumoto, H. Umezawa, S. Seki and M. Tachiki, Phys. Rev. **B17** (1978), 2276.